GEOCHEMISTRY INTERNATIONAL, 2025, Vol. 70, No. 1, pp. 61–73

DIFFERENTIATION FEATURES OF ALKALINE ROCKS IN ILMEN MIASKITE MASSIF: NEW MINERALOGICAL AND GEOCHEMICAL DATA

©2025 E. S. Sorokina[a,*], E. V. Medvedeva[b], A. B. Nemov[b], M. A. Rassomakhin[b], and L. N. Kogarko[a]

[a]*Vernadsky Institute of Geochemistry and Analytical Chemistry Russian Academy of Sciences (GEOKHI RAS), Moscow, Russia*

[b]*South Urals Research Center of Mineralogy and Geoecology, Urals Br. Russian Academy of Sciences (SU FRC MG UB RAS), Miass, Russia*

**e-mail: esorokina@geokhi.ru*

Received March 28, 2024
Revised August 07, 2024
Accepted August 15, 2024

Abstract. The Ilmen miaskite massif located in the Southern Urals remains largely understudied from mineralogical and geochemical standpoints, while the theories of its formation are still debatable. The article presents new data on mineral associations of miaskite varieties and REE-rich minerals. Geochemical studies determined pyroxene-amphibole miaskites as the most promising variety on REE mineralization (REE content at ca.1500 μg/g). These rocks showed distinct positive Nb anomalies combined with a negative Pb anomaly. The temperatures of feldspar exsolution indicate their following formation sequence within miaskite varieties (from higher temperature to lower temperature ones): pyroxene-amphibole miaskite → garnet-amphibole miaskite → amphibole miaskite → biotite miaskite.

Keywords: *Ilmen-Vyshnevogorsk alkaline complex, geochemistry and mineralogy of REE, pyrochlore*

DOI: 10.31857/S00167525250103e6

INTRODUCTION

The Ilmen miaskite massif (IMM) is located in the southern part of the Ilmen-Vyshnevogorsk Complex (IVC) of the Southern Urals. The massif is composed predominantly of special varieties of nepheline syenites with agpaitic coefficient <1, named miaskites because of their localization near Miass, Chelyabinsk region. The presence of these alkaline rocks significantly affects the mineral diversity of the complex, including the presence of REE mineralization in the area. Studies in recent years (structural, mineralogical, and petrogeochemical, Medvedeva et al., 2013; Nemov et al., 2017) have shown the absence of preserved signs of an ancestral magmatic process in the miaskites, the complexity of the formation history, and the distinct influence of metamorphic processes. Nevertheless, the massif remains significantly understudied from mineralogical and geochemical standpoints, while theories of its formation remain largely debated. Thus, there are several hypotheses for the formation of nepheline syenites-miaskites of the IVC: anatectic, under the influence of mantle fluids (Levin, 1974); riftogenic magmatic (Kramm et al., 1983; Rusin et al., 2006b). Therefore, the aim of the work was to determine the genetic features of miaskite formation by means of mineralogical and geochemical studies, as well as to identify the potential for REE and rare-metal mineralization.

In this publication, nepheline syenite-miaskite varieties of the IMM were identified. This work presents the first precision geochemical characterization of these miaskites, identification of novel REE minerals in the Ilmen Massif, and reconstruction of their formation sequence.

GEOLOGICAL FEATURES

Alkaline rocks of the IVC are represented by two miaskite massifs – Ilmen in the south (IMM)

and Vishnevogorsk in the north. The two massifs are connected by the Central Alkaline Belt (CAB) of intensely dislocated alkaline rocks of nepheline-syenite composition. The latter include carbonatite bodies, metasomatites, as well as boudinaged metamorphic and igneous rock bodies. The Ilmen Massif has a teardrop shape measuring 18 × 4.5 km (Fig. 1). The massif is heterogeneous in composition: in the west it is composed predominantly of amphibole miaskites, while in the east biotite miaskites are localized. The central part of the IMM is represented by alternating beds of miaskite and phenitized rocks. Within the IMM there are bodies of 0.1 m – 0.5 × × 0.5 – 10 m of pyroxene-amphibole ('sanduites' –

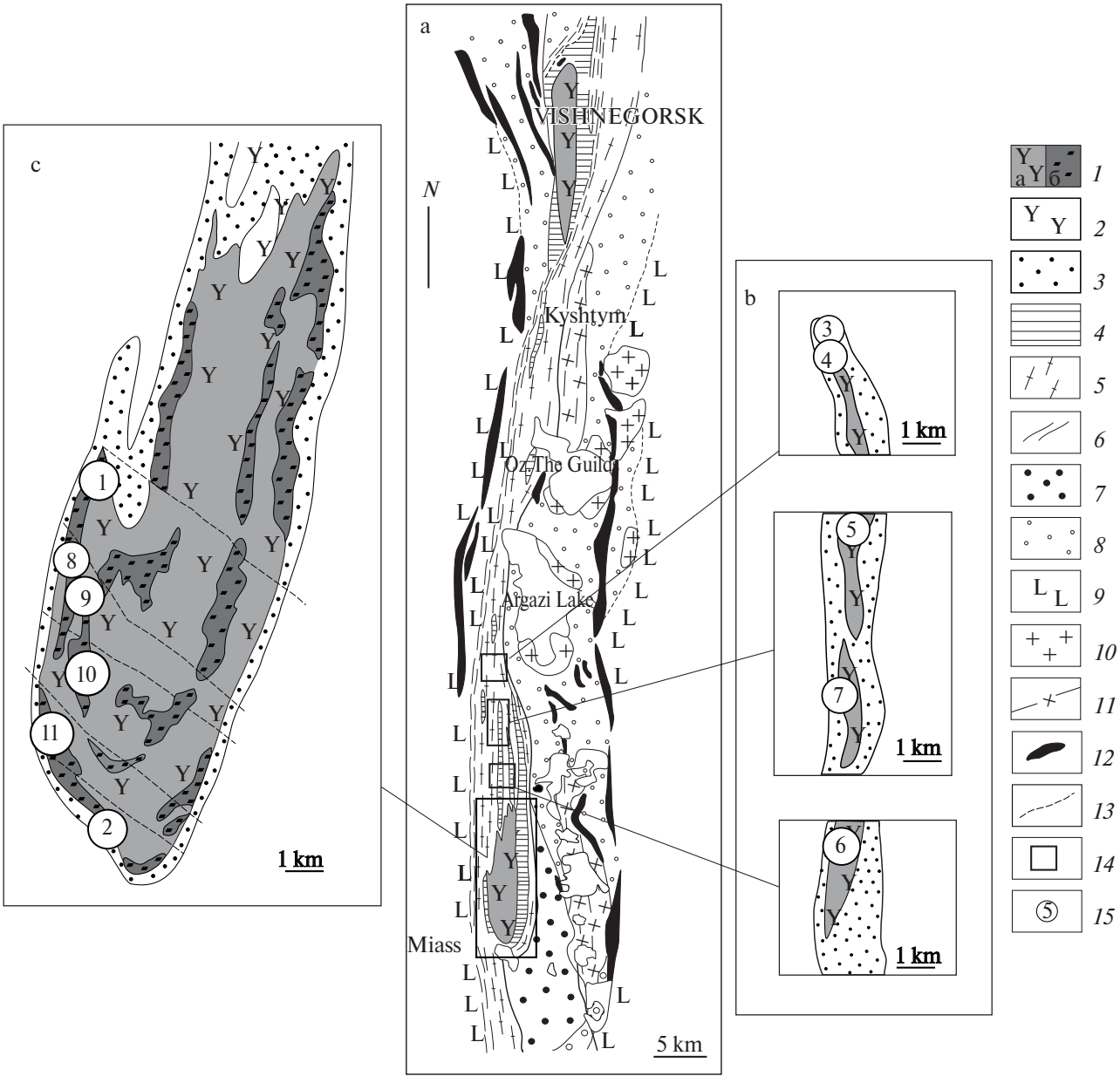

Fig. 1. Scheme of geologic structure: a) IVC; b) IMM; c) CAB. *1* – miaskites (O_2): (a) biotite, (b) amphibole; *2* – syenites (O_2); *3* – phenites; *4* – Selyankinskaya series amphibole-gneiss-plagiomigmatite ($Ar–Pt_1$); *5* – syenitic and granitic blastomylonites ($P_2–T_1$?); *6* – mylonites of the Kyshtym thrust-strike-slip zone; *7* – Yelanchik Formation: plagioclase schists and migmatites; *8* – Saitovo meta-terrigenous series; *9* – greenschist-facies sedimentary-volcanic complexes of the West Magnitogorsk zone and Aramil-Sukhtelinsk zone; *10* – Uvil'da monzonite-granite complex (Late Paleozoic, Pz_3); *11* – gneissic granites of the Kisegach complex; *12* – meta-ultramafic rocks; *13* – tectonic faults; *14* – study areas; *15* – sampling locations.

mainly in the western part) and garnet-amphibole ("firsites") miaskites, and less frequently vein-like bodies of albite miaskites. The boundaries between rock varieties are gradual, but sometimes sharp transitions between "sandyites" or albite miaskites and host amphibole miaskites are recorded. The bodies of "sandyites" and "firsites" occur conformably with the schistosity in the host miaskites. Whereas albite miaskites are subordinate to the gneiss and, consequently, to the strike of the host rocks (Levin et al., 1997)

Isotopic-geochemical studies of miaskites indicate two stages of their formation. The first stage 460–430 Ma is the time of formation or introduction of miaskite-carbonatite magma (Rb–Sr dating, Kramm et al., 1983). At the same time, the obtained values of $^{87}Sr/^{86}Sr_{(450\ Ma)}$ and $\varepsilon Nd_{(450\ Ma)}$ indicate a mantle source of fluids involved in the formation of IMM miaskites (Nedosekova, 2012; Sorokina et al., 2021). The second stage 330–220 Ma was collisional processes associated with the emplacement of the regional shear zone (Kramm et al., 1983; Nedosekova, 2012; Krasnobaev et al., 2016; Sorokina et al., 2021). The last geological stage led to metamorphic changes affecting almost all rocks of the IMM (Levin, 1974), and is also associated with the formation of syenite and miaskite pegmatite bodies with REE and rare-metal mineralization (Sorokina et al., 2017).

MATERIAL AND METHODS

During the field work, the authors collected samples of miaskites from different areas of the IMM (28 samples). The chemical composition of rocks was analyzed in SRF South Urals Research Center of Mineralogy and Geoecology of the Urals Branch of the Russian Academy of Sciences using methodological recommendations NSAM No. 138-X, NSAM No. 50-X, NSAM No. 172-C, NSAM № 502-C, NSAM No. 118-X, NSAM No. 120-X, NSAM No. 197-X. The quantitative values of the main petrogenic elements for SGD-2a, used as a standard sample for measurements, varied within the error from the certified values for this material. Geochemical data for the samples were obtained by inductively coupled plasma mass spectrometry (ICP-MS) in the laboratory of GEOKHI RAS on the Element-XR mass spectrometer (Thermo Finnigan). Sample preparation was preliminarily carried out using the acid decomposition technique (Bychkova et al., 2016). Three standard samples were used for quality control of ICP-MS measurements – STM-2, BHVO-2, BCR-2. Measurement errors of internal standards did not exceed 15–20% of their certified values according to the GeoRem database (http://georem.mpch-mainz.gwdg.de/). The chemical composition of minerals was investigated at the Institute of Mineralogy in Miass using electron microscope Vega-3 TESCAN with energy-dispersive spectrometer OXFORD instruments X-act. Imaging parameters: voltage – 20 kV, current – 500 pA, beam diameter – 5 μm. Standard samples were represented by MINM25-53 standards of natural and synthetic compounds manufactured in "ASTIMEX Scientific Limited" and "Microanalysis Consultants Ltd.". The measurement error of most elements in the standard samples did not exceed 0.2 wt. % (up to 0.3 wt. % for Fe, Nd, Ce, La, Nb, Pr, Sr and Zr).

RESULTS AND DISCUSSION

Mineral composition and sequence of miaskite formation

Six varieties of nepheline syenite-miaskites have been identified in the IMM area: pyroxene-amphibole miaskites – "sandyites", biotite miaskites, garnet-amphibole miaskites ("firsites"), amphibole miaskites, amphibole-biotite miaskites and albite miaskites (plagiomiaskites).

Amphibole, biotite, and amphibole-biotite miaskites are quite similar in mineral assemblage. They contain K-feldspar (up to 45 vol. %) and nepheline (up to 30 vol. %). The differences between them are variations of biotite (up to 20–30 vol. %) and amphibole (15–30 vol. %) contents in biotite-rich and amphibole-rich miaskites, respectively. Amphibole in them are represented predominantly by taramite, less frequently by hastingsite. Additionally, albite (up to 15 vol. %) was found in biotite-amphibole and biotite miaskites. The rocks of these varieties in the CAB area are significantly mylonitized and altered by later processes of albitization, carbonatization, and zeolitization (Levin et al., 1997). It is important to note that biotite marks the planes of mylonitization, while plagioclase grains are oriented subordinately to the striation (Medvedeva et al., 2013). In the IMM area, mylonitized varieties are much less common. These IMM and CAB varieties are similar in mineral composition to nepheline syenites found in the Eastern Ghats of India (Bhattacharya and Kar, 2004).

The composition of "sandyites" is dominated by pyroxene (aegirine, up to 50 vol. %) and amphibole (taramite, up to 35 vol. %), combined with smaller amounts of K-feldspar (up to 10 vol. %), plagioclase (up to 5 vol. %) and nepheline (up to 5 vol. %). The rocks are mylonitized, pyroxene is absent in segments of more intensely manifested deformation, but the amount of biotite increases (Nemov et al., 2017). Sandyites of the IMM are similar in mineral

assemblage with pyroxene-amphibole alkaline rocks of the Chernigov complex of the Ukrainian Shield (Glevassky and Krivdik, 1981) and British Columbia in Canada (Pell, 1987).

"Firsites" have gradual transitions to amphibole miaskites, slightly differing from the latter in structure and mineral composition. Thus, in addition to K-feldspar (30–40 vol. %), plagioclase (up to 30 vol. %), nepheline (up to 20 vol. %) and amphibole (taramite, sometimes hastingsite up to 10 vol. %), they contain garnet of the grossular-andradite series (up to 5 vol. %).

Albite miaskites occur both in the CAB and in the IMM, often in the endocontact zone among amphibole, amphibole-biotite, and biotite miaskites. Albite in the amount of 40–90 vol. % is represented by tabular grains, which in mylonitized varieties is represented by porphyroclasts (Levin, 1997). The latter are surrounded by smaller fragments of recrystallized albite grains and xenomorphic grains of homogeneous K-feldspar (up to 8 vol. %), nepheline (up to 20 vol. %) and biotite (up to 5 vol. %).

The matrix of all varieties of miaskites is composed of feldspars, so these minerals were used to calculate the exsolution temperatures (solvus) of these minerals in these rocks. Thus, the exsolution temperatures in K-felspar-plagioclase (microcline- pertite) pairs calculated from the Putirka (2008) two-feldspar thermometer varied slightly with pressure (Table 1). The obtained values indicate the following sequence of microcline-pertite pair formation in miaskite varieties: "sandyites" (~540°C) → "firsites" (500°C) → → amphibole miaskites (492°C) → biotite miaskites (465°C).

In addition to alkaline elements, factors that reduce the temperature in a magmatic system include the presence of H_2O, F and CO_2 (Marks and Markl, 2017), often present in REE concentrator minerals of miaskites (see below).

REE concentrator minerals in miaskite varieties

As a rule, varieties of miaskites are characterized by a different set of REE concentrator minerals. Thus, titanite-allanite association is characteristic of "sandyites" and amphibole miaskites. In the latter, monazite-(Ce) and ankylite may be additionally present. Whereas in biotite miaskites and "firsites" pyrochlore mineralization with secondary nioboaeshynite was found. Apatite group minerals are present in almost all varieties of miaskites (described earlier in Nedosekov et al. 2010, Table 2).

Titanite-allanite association. Titanite is associated with amphibole (taramite), it contains Al_2O_3 up to 5.6 wt. % and F up to 1.2 wt. % (Table 2). The mineral is often zonal with variable amounts of FeO and Nb_2O_5 (up to 1.1 wt. %). Inclusions of ilmenite, rutile (amount of Nb_2O_5 up to 5.8 wt. %) and zircon are observed in titanite.

Allanite-(Ce) associates with nepheline and is characterized by the presence of La_2O_3 (up to 9.7 wt. %, Table 2) and Ce_2O_3 (up to 10.5 wt. %). Additionally, up to 1 wt % Pr_2O_3, Nd_2O_5, and ThO_2 were found in this mineral from amphibole miaskites. Allanite is often replaced by bastnäsite (Ce_2O_3 + La_2O_3 up to 50 wt. %, Table 2). Additionally, a mixture of REE silicates and carbonates (Ce_2O_3 up to 40 wt. %, ThO_2

Table 1. Chemical composition of microcline-pertite pairs with exsolution temperatures (solvus) in miaskite varieties

Rock	Mineral pair	Oxide						Amount	*T*, solvus	*P*, GPa
		Na_2O	Al_2O_3	SiO_2	K_2O	CaO	BaO			
Sandyit	K-feldspar	5.6	19.2	65.3	8.2	UDL	1.1	99.3	539	15
	plagioclase	12.0	19.4	68.1	UDL	UDL	UDL	99.6		
Firsite	K-feldspar	2.1	18.1	65.7	13.7	UDL	UDL	99.6	500	15
	plagioclase	11.1	20.1	67.3	0.1	1.0	UDL	99.6		
Amph. miaskite	K-feldspar	1.4	18.6	66.1	14.8	UDL	UDL	100.9	492	15
	plagioclase	10.4	20.8	67.7	0.1	1.9	UDL	101.1		
Biot. miaskite	K-feldspar	0.9	18.8	64.9	15.1	UDL	UDL	99.8	465	15
	plagioclase	10.6	20.3	67.4	0.6	1.0	UDL	99.9		

Notes. UDL – under detection limit.

Table 2. REE concentrator minerals detected in the studied samples

Breed	Samples for EMPA	Apatite	Titanite	Allanite	Silicate of REE	Bastnäsite	Remondite	Pyrochlore	Nioboae-shynite	Monazite
Sandyit	AL6a-13	+	+	+	+					
Amphibole miaskite	Nm9-13		+	+		+	+			+
	Al 1-13		+							
Biotite miaskite	Nm4-13	+						+	+	+
Firsite	Al6-13							+		
	F-85			+						

Notes. Rocks with titanite-allanite mineral association are highlighted in light gray, rocks with pyrochlore mineral association are highlighted in dark gray.

up to 11 wt. %, Nd_2O_3 up to 3 wt. %) is present, difficult to diagnose with the research methods used, including a mineral in which the REE:(Na + Ca) ratio suggests remondite (contains Ce_2O_3 + La_2O_3 up to 40 wt. %, Na_2O – 8.1 wt. %, CaO – 6.6 wt. %, SrO – 5.1 wt. %).

Fluorapatite was found in assemblage with biotite and calcite. The mineral is enriched in REE (Table 3) and contains La_2O_3 (up to 0.9 wt. %), Ce_2O_3 (up to 1.7 wt. %), Nd_2O_3 (0.4 wt. %) and SrO (1.7 wt. %).

Pyrochlore association. Minerals of the pyrochlore group were found in the K-feldspar-albite matrix of miaskites. Three minerals are present – Hydroxycalciopyrochlore, oxycalciopyrochlore, and fluornatropyrochlore (Table 4). The latter was first discovered by the authors on the territory of the IMM in the corundum miaskite pegmatite No. 210 (Rassomakhin et al., 2020). Pyrochlore is often zonal in composition. It is important to note that hydroxycalciopyrochlore contains the highest amount of Nb_2O_5 (up to 71.4 wt. %), whereas fluornatropyrochlore accumulates more REEs: Ce_2O_3 up to 9.2 wt. %, Nd_2O_3 up to 3.2 wt. %, La_2O_3, 0.9 wt. % Pr_2O_3. The content of ThO_2 in the minerals of the pyrochlore group reaches 2 wt. %, and also in their grains often observed areas with a gradual increase in the amount of SiO_2 up to 12.3 wt. % with the possible formation of a new mineral phase corresponding to the composition of komarovite (Fig. 2, for an accurate diagnosis of the mineral species requires additional studies).

Nioboaeshynite-(Ce) is found in association with albite exclusively in biotite miaskites. The mineral contains Nb_2O_5 up to 36.2 wt. %, Ce_2O_3 up to 21.2 wt. %, $TiO_2$20.2 wt. %, La_2O_3 up to 6.3 wt. %, Nd_2O_3 up to 7 wt. % and Pr_2O_3 up to 2.2 wt. % (Table 4). Its chemical formula converted to 3 cations is as follows: $(Ce_{0.49}Nd_{0.159}Ca_{0.119}La_{0.147}Pr_{0.05})_{(0.965)}(Nb_{1.037}Ti_{0.963}Fe_{0.028})_{2.028}(O,OH)_6$.

Monazite-(Ce) was found in the K-feldspar-biotite matrix of miaskites. The mineral contains Ce_2O_3 up to 33.5 wt. %, La_2O_3 up to 28.5 wt. %, Nd_2O_3 up to 4.5 wt. %, Pr_2O_3 up to 1.8 wt. % and ThO_2 up to 4.3 wt. % (Table 3).

Thus, the evolution of the composition of miaskites with pyrochlore mineral association is expressed in the gradual accumulation of Na, Si, Sr, Th, and LREE. This fact is caused by the change in the composition of pyrochlore minerals (from oxycalciopyrochlore to fluornatropyrochlore) and then by their replacement by a mineral close in composition to komarovite at later stages. This geochemical trend is characteristic of pyrochlore group minerals from late associations of Proterozoic alkaline-ultrabasic intrusions of the Kola Peninsula (Sorokhtina et al., 2019).

Geochemical features of miaskite varieties

All studied samples of miaskites are characterized by low agpaitic coefficient AI (0.6–0.7, Table 5) and high aluminum saturation index ASI (1–1.5).

Among miaskite varieties, *pyroxene-amphibole varieties* ("sandyites") are the most promising for rare-earth mineralization: REE content in them reaches 1570 μg/g, which is close to the average REE amount in the Lovozero alkaline massif (~2500 μg/g,

Table 3. Composition of REE concentrator minerals with titanite-allanite mineral association

Oxide	Titanite		Allanite-(Ce)		Bastnäsite-(Ce)		Fluorapatite	
	NM9-13	AL6a-13	NM9-13	AL6a-13	NM9-13	NM9-13	NM4-13	AL6a-13
Al_2O_3	5.6	5.0	17.4	17.9	3.7	4.3	UDL	UDL
SiO_2	32.3	31.7	33.5	35.0	8.3	9.3	0.2	UDL
CaO	29.6	28.3	12.4	5.8	4.2	4.7	51.8	52.4
TiO_2	31.1	32.3	0.4	1.3	UDL	0.8	UDL	UDL
MnO	UDL	UDL	0.8	0.9	UDL	UDL	UDL	UDL
FeO	0.6	1.3	14.8	9.3	2.9	3.4	UDL	0.7
SrO	UDL	UDL	UDL	UDL	UDL	UDL	UDL	1.7
La_2O_3	UDL	UDL	9.7	5.9	23.4	25.3	0.9	0.5
Ce_2O_3	UDL	UDL	10.3	5.8	23.5	23.4	1.7	0.7
Nb_2O_5	0.8	0.3	UDL	UDL	UDL	UDL	UDL	UDL
Nd_2O_3	UDL	UDL	0.6	UDL	1.1	UDL	0.4	UDL
Pr_2O_3	UDL	UDL	0.6	UDL	1.1	UDL	UDL	UDL
ThO_2	UDL	UDL	1.2	UDL	2.1	2.2	UDL	UDL
P_2O_5	UDL	UDL	1.0	1.0	1.4	1.6	40.2	40.4
F	1.2	1.1	UDL	UDL	1.6	1.4	2.5	2.9
Amount	101.5	100.2	101.9	84.4	72.3	76.3	98.2	99.2
Restated to:								
	5 anions		13 anions		1 cation		13 anions	
Al	0.215	0.193	2.131	2.304	0.115	0.112	0.000	0.000
Si	1.046	1.039	3.485	3.823	0.215	0.207	0.014	0.000
Ca	1.027	0.994	1.385	0.678	0.118	0.112	4.906	4.922
Ti	0.757	0.796	0.032	0.110	0.000	0.013	0.000	0.000
Mn	0.000	0.000	0.053	0.061	0.000	0.000	0.000	0.000
Fe	0.015	0.036	1.285	0.849	0.064	0.063	0.000	0.048
Sr	0.000	0.000	0.000	0.000	0.000	0.000	0.000	0.080
La	0.000	0.000	0.371	0.237	0.225	0.208	0.028	0.017
Ce	0.000	0.000	0.392	0.232	0.224	0.191	0.056	0.023
Nb	0.012	0.004	0.000	0.000	0.000	0.000	0.000	0.000
Nd	0.000	0.000	0.044	0.000	0.019	0.017	0.014	0.000
Pr	0.000	0.000	0.024	0.000	0.011	0.000	0.000	0.000
Th	0.000	0.000	0.023	0.024	0.009	0.008	0.000	0.000
P	0.000	0.000	0.000	0.000	0.000	0.000	3.010	2.998
F	0.120	0.110	0.000	0.000	0.133	0.101	0.707	0.790
OH Calc	0.000	0.000	0.000	0.000	0.000	0.000	0.293	0.210

Notes. UDL – under detection limit.

Table 4. Composition of REE concentrator minerals with pyrochlore association

Oxide	Hydroxycalcio-pyrochlore		Oxycalciopyrochlor			Fluornatropyrochlor	Nioboaeshynite-(Ce)	Monazite-(Ce)	
	NM4-13		AL6-13			NM4-13	NM4-13	NM9-13	NM4-13
Na_2O	UDL	UDL	6.1	6.2	6.1	6.8	UDL	UDL	UDL
SiO_2	0.6	0.8	0.3	0.3	0.5	0.6	0.6	0.6	0.2
P_2O_5	UDL	UDL	UDL	UDL	UDL	UDL	UDL	29.6	30.4
CaO	15.2	8.2	19.0	18.6	18.5	11.3	1.8	0.5	UDL
TiO_2	5.3	8.5	7.3	7.3	7.3	8.3	20.2	UDL	UDL
MnO	0.4	1.4	UDL	UDL	UDL	UDL	UDL	UDL	UDL
FeO	3.2	1.4	0.2	UDL	UDL	0.3	0.5	UDL	0.4
SrO	UDL	UDL	UDL	UDL	UDL	0.6	UDL	UDL	UDL
Y_2O_3	UDL	UDL	UDL	UDL	UDL	1.2	UDL	UDL	UDL
Nb_2O_5	71.4	61.4	59.6	59.3	59.1	52.7	36.2	UDL	UDL
La_2O_3	UDL	2.0	UDL	UDL	UDL	1.7	6.3	28.5	28.3
Ce_2O_3	1.9	7.6	0.7	0.6	0.7	9.2	21.2	32.0	33.5
Nd_2O_3	UDL	4.2	UDL	UDL	UDL	3.2	7.0	3.0	4.5
Ta_2O_5	1.0	1.5	UDL	UDL	UDL	1.5			
Pr_2O_3	UDL	0.5	UDL	UDL	UDL	0.9	2.2	1.6	1.8
ThO_2	UDL	UDL	1.6	1.9	1.6	UDL	UDL	4.3	UDL
UO_2	UDL	UDL	UDL	UDL	0.1	UDL	UDL	UDL	UDL
F	UDL	UDL	UDL	UDL		1.7	UDL	UDL	UDL
Amount	98.9	97.4	98.3	97.8	97.1	99.7	95.9	100.0	99.0
Calculated to:									
Cation (anion)	Nb + Ti + Ta + Fe = 2						Nb + Ti = 2	4 anions	
Na	0.000	0.000	0.727	0.746	0.728	0.859	0.000	0.000	0.000
Si	0.030	0.042	0.020	0.021	0.032	0.036	0.035	0.023	0.007
P	0.000	0.000	0.000	0.000	0.000	0.000	0.000	0.982	1.004
Ca	0.830	0.492	1.248	1.235	1.233	0.791	0.119	0.019	0.000
Ti	0.205	0.358	0.335	0.341	0.341	0.411	0.963	0.000	0.000
Mn	0.013	0.051	0.000	0.000	0.000	0.000	0.000	0.000	0.000
Fe	0.138	0.065	0.010	0.000	0.000	0.017	0.028	0.000	0.014
Sr	0.000	0.000	0.000	0.000	0.000	0.021	0.000	0.000	0.000
Y	0.000	0.000	0.000	0.000	0.000	0.041	0.000	0.000	0.000
Nb	1.644	1.554	1.655	1.659	1.659	1.562	1.037	0.000	0.000
La	0.000	0.040	0.000	0.000	0.000	0.040	0.147	0.412	0.408
Ce	0.035	0.156	0.017	0.014	0.015	0.220	0.490	0.460	0.478
Nd	0.000	0.083	0.000	0.000	0.000	0.074	0.159	0.042	0.063
Ta	0.014	0.023	0.000	0.000	0.000	0.026	0.000	0.000	0.000
Pr	0.000	0.011	0.000	0.000	0.000	0.021	0.050	0.022	0.025
Th	0.000	0.000	0.022	0.027	0.022	0.000	0.000	0.038	0.000
U	0.000	0.000	0.000	0.000	0.002	0.000	0.000	0.000	0.000
F	0.000	0.000	0.000	0.000	0.000	0.361	0.000	0.000	0.000

Notes. UDL – under detection limit.

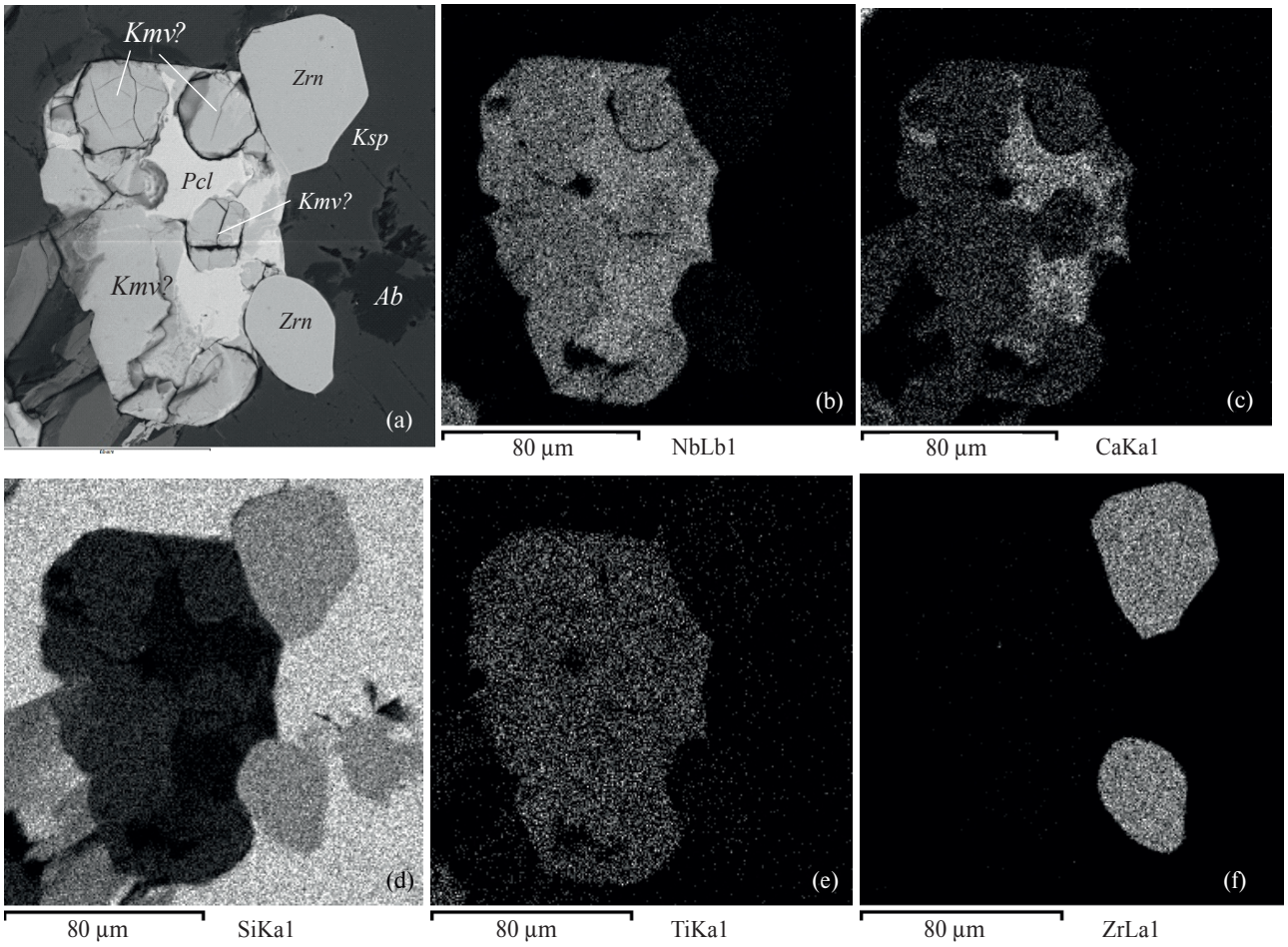

Fig. 2. Pyrochlore grains (Pcl) in association with zircon (Zrn), as well as with inclusions and aggregates with silicon-enriched niobium mineral close to komarovite (Kmv?): a – image in backscattered electrons, b–f – maps of Nb, Ca, Si, Ti and Zr contents. Ab – albite, Ksp – kalispar.

Table 5). In contrast to other varieties, bulk XRF analyses of "sandyites" showed their depletion of Al_2O_3 (~18 wt. %) and SiO_2 (~44 – 47 wt. %) with enrichment of TiO_2 (~3 wt. % – 3 times higher than in the Lovozero alkaline massif, Table 4), MgO (~2 wt. %), FeO (~9–10 wt. %) and CaO (~6–8 wt. %). Such features of the rocks are related to their mineral composition, where aegirine and taramite predominate with lower amounts of orthoclase-microcline (see above).

"Sandyites" are characterized by enrichment of LREE compared to HREE on the spectra normalized to chondrite, Eu anomaly is absent (Fig. 3). At the same time, the spectra show enrichment of these rocks in REE compared to other varieties of miaskites. This fact is due to high REE distribution coefficients in allanite-alkaline melt equilibrium. "Sandyites" are enriched with incompatible elements, show a distinct positive Nb anomaly and negative Pb anomaly on the spectra normalized to the primitive mantle (Fig. 3).

The other varieties of miaskites (*amphibole* and *biotite miaskites*, *"firsites"*), compared to 'sanduites', are characterized by higher contents of SiO_2 (~55–56 wt. %) and Al_2O_3 (~22–23 wt. % – higher than in the Lovozero massif) combined with lower values of TiO_2 (~0.3–0.8 wt. %), MgO (~0.2–0.4 wt. %), FeO (~1.6–2.2 wt. %) and CaO (~0.6–2.3 wt. %). The amount of REE varies in the range of 10–200 μg/g (the largest amount is contained in "firsites" – 150–200 μg/g). At the same time, the content of other ore elements such as Sr, Ba, Nb and Pb in individual samples of miaskites is higher than their average value in the Lovozero massif (see Table 5). These varieties contain less incompatible elements (negative Ba, Th, La, Ce, Nd anomalies) compared to "sandyites". However, they show pronounced positive Nb and Pb anomalies. The positive Pb anomaly is probably related to the contamination of these varieties of miaskites by crustal rocks (Fig. 3).

Table 5. Chemical composition of the studied samples of miaskite varieties

Oxide, wt. %	NM 9-13	AL1-13	NM-1-13	NM3-13	NM4-13	NM-6-13	miask-1	AL7-13	NM7-13	AL6a-13	Ф-85	AL-6-13	Lovozero
	Amph. miaskite		Biotite miaskite					Sandyites			Firsites		
SiO_2	55.3	56.6	55.1	56.0	54.7	55.1	58.7	46.6	43.6	–	–	56.4	53.5
TiO_2	0.6	0.3	0.7	0.8	0.7	0.5	0.9	2.7	3.1	–	–	0.3	1.1
Al_2O_3	22.9	22	21.7	22.8	23.2	22.7	22.8	17.6	18.1	–	–	22.7	17.4
Fe_2O_3	1.1	2.1	1.2	0.6	0.5	0.7	2.3	5.0	5.8	–	–	2.0	–
CaO	1.7	1.5	2.3	0.9	1.5	1.2	0.6	5.7	8.2	–	–	1.6	1.2
FeO	1.7	1.9	2.2	2.1	2.2	2.2	–	5.7	4.2	–	–	1.6	5.44
MnO	0.1	0.3	0.1	0.1	0.1	0.1	0.1	0.7	0.7	–	–	0.3	0.34
MgO	0.3	0.2	0.4	0.3	0.3	0.3	0.3	2.4	1.9	–	–	0.2	1.0
Na_2O	7.6	7.0	8.0	6.9	7.6	7.4	9.0	6.7	9.0	–	–	7.4	10.9
K_2O	7.3	6.9	5.5	7.4	7.2	6.9	4.4	5.1	3.1	–	–	6.8	5.9
H_2O^-	0.1	0.1	0.2	0.1	0.1	0.3	–	UDL	0.1	–	–	0.1	–
LOI	0.9	0.5	2.6	1.6	1.4	2.1	0.6	1.1	1.4	–	–	0.6	–
P_2O_5	0.1	UDL	0.3	0.2	0.2	0.2	0.03	0.4	0.6	–	–	0.1	0.2
Amount	99.6	99.55	100.3	99.8	99.5	99.6	100.4	99.9	99.8	–	–	99.9	–
$Na_2O + K_2O$	14.8	13.92	13.5	14.3	14.8	14.3	13.3	11.8	12.1	–	–	14.2	16.8
AI	0.6	0.6	0.6	0.6	0.6	0.6	0.6	0.7	0.7	–	–	0.6	1
ASI	1.4	1.4	1.4	1.5	1.4	1.5	1.6	1.0	0.9	–	–	1.5	1
Li	3.35	2.57	3.49	2.97	3.99	7.09	3.9	18.04	6.24	13.58	1.44	2.00	55
Sc	0.273	0.275	0.667	0.330	0.259	0.219	–	4.03	3.034	3.92	0.217	0.067	–
V	33.4	39.8	56.3	57.5	58.2	49.3	31	193	191	215	28.7	49.2	108
Cr	15.4	20.0	18.3	13.9	23.5	8.17	70	88.1	7.52	3.38	19.3	8.73	27.8
Co	1.17	1.48	2.09	1.71	1.45	1.19	1.7	9.33	7.70	10.4	1.30	1.11	–
Cu	8.30	11.41	14.5	24.5	13.5	7.90	13	16.7	7.14	14.1	16.4	8.76	11
Zn	130	62.7	48.1	49.3	41.6	267	8.6	445	325	349	139	74.8	210
Rb	67.5	69.4	31.0	42.3	29.8	66.6	38	114	77.9	86.3	70.7	82.7	230
Sr	194	264	1865	672	590	390	715	829	512	1594	1447	523	610
La	43.6	5.59	10.0	7.753	9.035	1.771	3.8	131	290	317	66.9	36.7	–
Ce	68.9	13.7	24.4	17.0	21.0	3.7	8.7	305	543	690	86.4	72.4	–

Table 5. (End)

Oxide, wt. %	NM 9-13	AL1-13	NM-1-13	NM3-13	NM4-13	NM-6-13	miask-1	AL7-13	NM7-13	AL6a-13	Ф-85	AL-6-13	Lovozero
	Amph. miaskite		Biotite miaskite					Sandyites			Firsites		
Pr	6.56	1.88	3.00	2.21	2.73	0.517	0.91	32.1	51.0	75.3	7.13	7.07	–
Nd	18.5	6.20	11.6	7.6	9.5	1.83	3	104	159	258	19.7	19.0	–
Sm	2.24	0.922	2.11	1.08	1.37	0.344	0.64	14.7	21.4	37.8	2.35	1.96	–
Eu	0.653	0.289	1.36	0.485	0.510	0.196	0.57	4.38	5.77	11.6	0.986	0.528	–
Gd	2.89	1.006	1.95	1.15	1.44	0.332	0.51	16.2	24.7	39.0	3.22	2.77	–
Tb	0.346	0.161	0.273	0.158	0.203	0.049	0.079	2.04	2.87	4.92	0.348	0.281	–
Dy	1.73	0.960	1.36	0.813	1.013	0.274	0.39	9.94	14.0	23.0	1.89	1.41	–
Ho	0.326	0.225	0.239	0.157	0.185	0.060	0.085	1.70	2.28	3.67	0.315	0.250	–
Er	1.06	0.923	0.713	0.493	0.580	0.173	0.26	5.35	7.47	11.2	1.03	0.966	–
Tm	0.153	0.177	0.094	0.066	0.074	0.026	0.047	0.689	0.959	1.31	0.136	0.161	–
Yb	0.875	1.45	0.571	0.402	0.455	0.101	0.32	4.38	6.24	7.87	0.777	1.34	–
Lu	0.152	0.312	0.096	0.066	0.072	0.026	0.048	0.693	1.03	1.13	0.128	0.284	–
Y	6.44	4.98	4.88	2.93	3.39	1.01	1.6	42.4	58.7	91.9	8.80	5.85	–
Zr	93.6	60.3	7.82	13.1	7.83	18.1	81	483	544	477	45.1	66.0	3480
Nb	123	937	201	117	114	147	726	444	496	435	73.8	220	696
Mo	5.65	0.884	0.658	1.16	1.32	0.411	0.86	0.857	1.51	2.04	15.9	0.708	1.7
Ba	152	21.4	3107	781	446	358	3037	983	230	3128	1306	39.7	700
Hf	3.01	2.51	0.375	0.528	0.286	0.387	1.4	11.1	12.4	12.3	1.34	2.46	83
Ta	5.41	7.05	7.90	5.43	5.22	5.35	23	15.3	20.3	30.7	3.15	3.84	60
W	0.728	0.410	0.227	0.258	0.249	0.285	–	0.231	0.232	0.231	0.224	0.172	–
Tl	0.312	0.191	0.096	0.161	0.148	0.404		0.159	0.146	0.092	0.151	0.225	–
Pb	14.8	1.91	7.90	9.51	16.3	13.6	4.1	14.6	6.60	17.7	49.1	5.88	14.6
Th	11.8	4.80	0.210	0.653	1.22	6.48	7	17.4	34.3	53.5	13.5	8.24	35
U	1.41	0.662	1.79	0.447	1.10	4.19	6.9	1.83	2.63	2.12	2.66	0.690	16.1
Ce/Pb	4.66	7.19	3.09	1.78	1.29	0.27	2.12	20.9	82.2	39.0	1.76	12.3	–
Nb/U	87.7	1416	112	262	104	35.0	105.2	242	189	205	27.8	319	–
La/Yb	49.8	3.85	17.6	19.3	19.8	17.6	11.88	29.9	46.5	40.2	86.1	27.4	–
ΣREE	154	39	63	42	52	11	21	675	1188	1574	200	151	2500

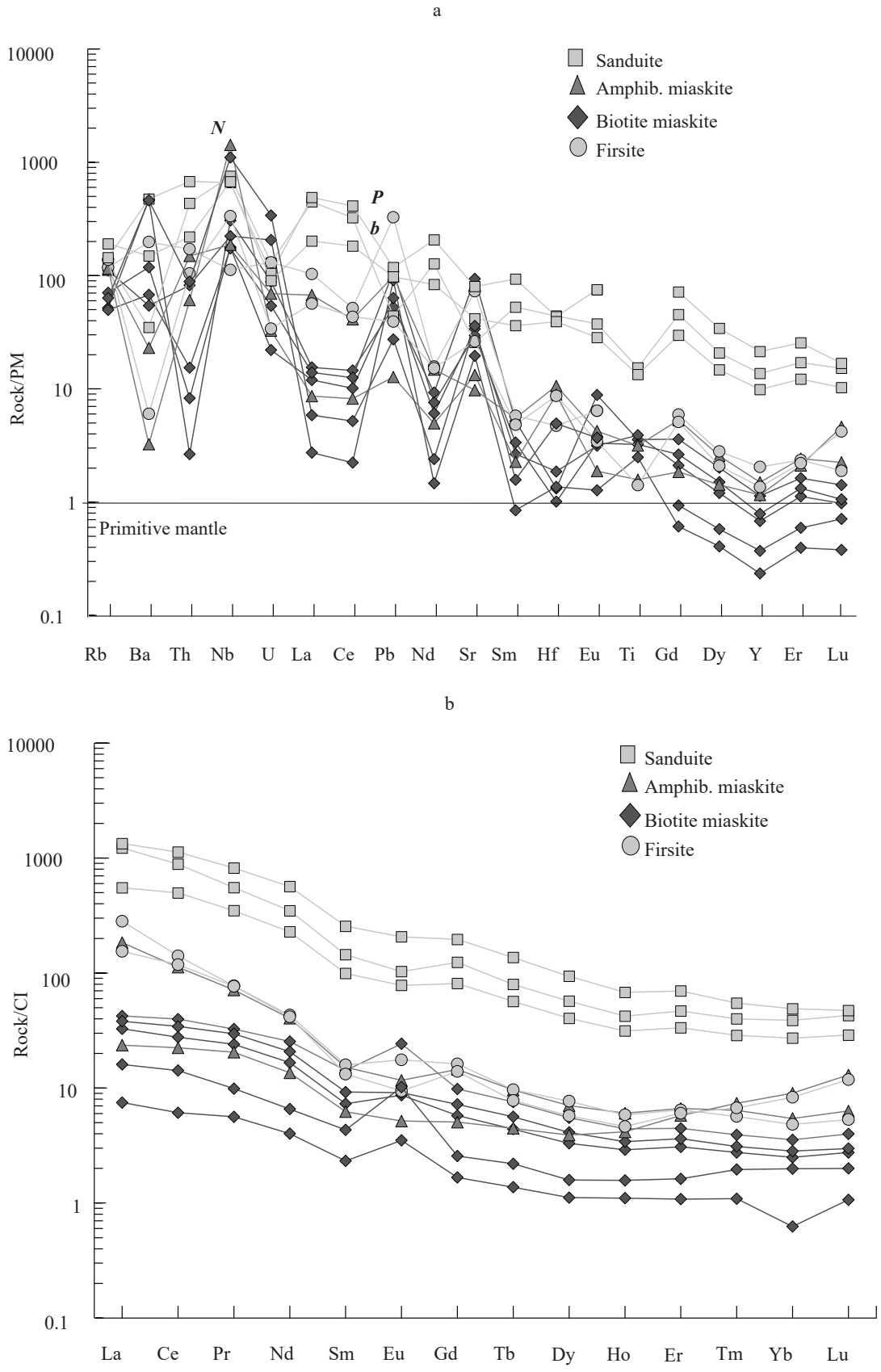

Fig. 3. Distribution diagrams of the contents of incompatible elements in IMM miaskites: a – normalized to primitive mantle; b – normalized to CI chondrite.

On spectra normalized to chondrite, these varieties, as well as "sandyites", are characterized by enrichment of LREE compared to HREE. However, unlike the latter, they often contain a positive Eu anomaly (Fig. 3), probably associated with the formation of plagioclase in the magmatic melt. At the same time, biotite miaskites as the lowest-temperature varieties contain less REE compared to other varieties (Fig. 3).

CONCLUSION

1. For the first time, high-precision geochemical data were obtained for all miaskite varieties. Among these, the pyroxene-amphibole variety ("sandyites") contains the highest REE concentrations (up to 1,570 μg/g), making it the most promising rock type for rare-earth mineralization in the Ilmen Massif region;

2. Chemical composition of "sandyites" shows their depletion of Al_2O_3 and SiO_2 with enrichment of TiO_2, MgO, FeO and CaO compared to other varieties of miaskites, this reflects their mineral composition comparable to that of pyroxene-amphibole rocks of the Ukrainian Shield and British Columbia in Canada.

3. "Sandyites" show distinct positive Nb anomaly and negative Pb anomaly on spectra normalized to primitive mantle. Amphibole and biotite miaskites and “firsites” have positive Nb and Pb anomalies. The positive Pb anomaly is probably due to the contamination of these varieties of miaskites with crustal rocks;

4. It was found that varieties of miaskites have characteristic associations of REE concentrator minerals. Thus, titanite-allanite association is characteristic for "sandyites" and amphibole miaskites. Whereas pyrochlore mineralization was found in biotite miaskites and “firsites”;

5. The formation temperatures of feldspars composing the matrix of miaskites indicate the following sequence of their formation (from higher-temperature to lower-temperature varieties): "sandyites" → "firsite" → → amphibole miaskites → biotite miaskites.

ACKNOWLEDGEMENTS

The authors are grateful to colleagues from GEOCHI RAS for assistance in sample preparation and analysis of the material – Dr. M.O. Anosova, D.A. Banaru and S.Y. Lapshin. The authors also thank Corresponding Member of RAS I.V. Pekov, Dr. V.A. Muftakhov, Scientific Editor Dr. O.A. Lukanin, and member of the Editorial Board of the Journal "Geochemistry" Dr. N.V. Sorokhtina for valuable comments on the earlier version of the manuscript.

FUNDING

This work was carried out within the state assignment of the Vernadsky Institute of Geochemistry and Analytical Chemistry of the Russian Academy of Sciences (GEOKHI RAS), a grant from the Ministry of Education and Science and SU FSC of Mineralogy and Geoecology RAS (No. 122040600006-1).

REFERENCES

1. *Bychkova Y.V., Sinitsyn M.Y., Petrenko D.B., Nikolaeva I.Y., Bugaev I.A., Bychkov A.Y.* (2016) Methodological features of trace element analysis of rocks by inductively coupled plasma mass spectrometry. *Bulletin of Moscow University*. 4(6). 56–63.
2. *Glevassky E.B., Krivdik S.G.* (1981) Precambrian carbonatite complex of the Azov region. Kiev: *Naukova Dumka*, 228 pp.
3. *Krasnobaev A.A., Valizer P.M., Busharina S.V., Medvedeva E.V.* (2016) Zirconology of miaskites from the Ilmensky Mountains (Southern Urals). *Geochemistry*. (9). 797–813.
4. *Krasnobaev A.A., Busharina S.V., Valizer P.M., Medvedeva E.V.* (2016) Zirconology of miaskites from the Ilmeny Mountains, South Urals. *Geochem. Int.* 54(9). 765–780.
5. *Levin V.Y.* (1974) The alkaline province of the Ilmensky-Vishnevy Mountains in the Urals. Moscow: *Nauka*, 223 p.
6. *Levin V.Y., Ronenson B.M., Samkov V.S., Levina I.A., Sergeev N.S., Kiselev A.P.* (1997) Alkali-carbonatite complexes of the Urals. Ekaterinburg: *Uralgeolcom*, 244 p.
7. *Medvedeva E.V., Kotlyarov V.A., Nemov A.B.* (2013) Mylonitized rocks of the Ilmen complex (Southern Urals). *Bulletin of the Institute of Geology of the Komi Scientific Center of the Ural Branch of the Russian Academy of Sciences*. 11(227). 7–10.
8. *Nedosekova I.L.* (2012) Age and sources of matter of the Ilmen-Vyshnevogorsk alkaline complex (Urals, Russia): geochemical and isotopic Rb–Sr, Sm–Nd, U–Pb, Lu–Hf data. *Lithosphere*. (5). 77–95.
9. *Nedosekova I.L., Vladykin N.V., Pribavkin S.V., Bayanova T.B.* (2009) Ilmen-Vyshnevogorsk miaskite-carbonatite complex: origin, ore bearing capacity, sources of matter (Ural, Russia). *Geology of Ore Deposits*. 51(2). 157–181.
10. *Nedosekova I.L., Udoratina O.V., Vladykin N.V., Pribavkin S.V., Gulyaeva T.Ya.* (2011) Petrochemistry and geochemistry of dyke ultrabasites and carbonatites

of the Chetlas Complex (Middle Timan). *Proceedings of the Institute of Geological Geology of the Ural Branch of the Russian Academy of Sciences*. 158. 122–130.

11. *Nemov A.B., Medvedeva E.V., Kotlyarov V.A.* (2017) Sandyites and rocks of monzonite composition of the Ilmen Miaskite Massif (Southern Urals). *Lithosphere*. 17(3). 87–101.

12. *Rassomakhin M.A., Kasatkin A.V.* (2020) Additions to the mineral cadastre of the Ilmensky Mountains. *Mineralogy*. 6(2). 18–26.

13. *Rassomakhin M.A., Sorokina E.S., Somsikova A.V.* (2020) Mineralogical and geochemical peculiarities of corundum miaskite pegmatite of Kopi No. 210 (Ilmensky Mountains, Southern Urals): preliminary results. *Mineralogy*. 6(2). 38–54.

14. *Rusin A.I., Krasnobaev A.A., Valizer P.M.* (2006a) Geology of the Ilmensky Mountains. *Proceedings of the conference "Geology and Mineralogy of the Ilmen Complex: Situation and Problems"*. Miass: *IGZ Ural Branch of the Russian Academy of Sciences*. 3–19.

15. *Rusin A.I., Krasnobaev A.A., Rusin I.A., Valizer P.M., Medvedeva E.V.* (2006b) Alkaline-ultrabasic association of the Ilmensky-Vishnevaya Mountains. *Proceedings of the conference "Geochemistry, Petrology, Mineralogy and Genesis of Alkaline Rocks"*. Miass: *Ural Branch of the Russian Academy of Sciences*. 222–227.

16. *Sorokhtina N.V., Belyatsky B.V., Antonov A.V., Lepekhina E.V., Kononkova N.N.* (2019) Phase and intra-phase heterogeneity of pyrochlore group minerals and age of formation of rare-metal mineralization of Vuoriyarvi massif, Kola Peninsula. *Proceedings of the Fersman Scientific Session of the GI KSC RAS*. 16. 559–564.

17. *Gerasimovsky V.I.* Chemical composition of rocks of the massif. In: *Geochemistry of the Lovozero Alkaline Massif* (Eds. *Gerasimovsky, Volkov, Kogarko, et al.*). Moscow: *Nauka*, 1966.

18. *Bhattacharya S., Kar R.* (2004) Alkaline intrusion in a granulite ensemble in the Eastern Ghats belt, India: Shear zone pathway and a pull-apart structure. *J. Earth Syst. Sci.* 113(1). 37–48.

19. *Hofmann A.W.* (1997) Mantle geochemistry: the message from oceanic volcanism. *Nature*. 385(6613). 219–229.

20. *Kramm U., Blaxland A.B., Kononova V.A., Grauert B.* (1983) Origin of the Ilmenogorsk-Vishnevogorsk nepheline syenites, Urals, USSR, and their time of emplacement during the history of the Ural fold belt: an Rb–Sr study. *J. Geol.* 91. 427–435.

21. *Marks M.A.W., Markl G.* (2017) A global review on agpaitic rocks. *Earth Sci. Rev.* 173. 229–258.

22. *Pell J.* (1987) Carbonatites, nepheline syenites, kimberlites and related rocks in British Columbia. *British Columbia Ministry of Energy, Mines and Petroleum Resources Open File Report 88*. 136 p.

23. *Putirka K.* (2008) Thermometers and Barometers for Volcanic Systems. In: *Minerals, Inclusions and Volcanic Processes* (Eds. *Putirka K., Tepley F.*). *Reviews in Mineralogy and Geochemistry*. *Mineralogical Society of America*. 69. 61–120.

24. *Sorokina E.S., Botcharnikov R., Kostitsyn Yu.A., Rösel D., Häger T., Rassomakhin M.A., Kononkova N.N., Somsikova A.V., Berndt J., Ludwig T., Medvedeva E.V., Hofmeister W.* (2021) Sapphire-bearing magmatic rocks trace the boundary between paleo-continents: a case study of Ilmen alkaline complex, Uralian collision zone of Russia. *Gondwana Res.* 92. 239–252.